ELSEVIER

Journal of Organometallic Chemistry 528 (1997) 35–45

Journal of Organometallic Chemistry

Donor/acceptor complexes containing ferrocenyl-pyridine ligands attached to a tungsten carbonyl centre: structural, spectroscopic and electrochemical properties

Sumika Sakanishi, David A. Bardwell, Samantha Couchman, John C. Jeffery *, Jon A. McCleverty *, Michael D. Ward *

School of Chemistry, University of Bristol, Cantock's Close, Bristol BS8 1TS, UK

Received 22 March 1996

Abstract

A series of ferrocenyl-pyridine ligands (Fc-L) in which a 4-pyridyl side-arm is attached to a ferrocenyl core via a conjugated linker has been attached to tungsten carbonyl cores, giving complexes of the type $[(Fc\text{-}L)W(CO)_5]$ (**1–6**) and $[(Fc\text{-}L)_2W(CO)_4]$ (**7** and **8**). Three of these complexes were characterised by X-ray crystallography. Complex **2**, $[\{Fc\text{–}C(Ph)=CH\text{–}C_5H_4N\}W(CO)_5]$: triclinic, $P\bar{1}$; $a = 9.329(4)$, $b = 12.115(3)$, $c = 12.745(3)$ Å; $\alpha = 66.66(2)$, $\beta = 71.87(2)$, $\gamma = 81.40(2)°$; $Z = 2$; 3230 unique data; $R_1 = 0.032$, $wR_2 = 0.090$. Complex **3**, $[\{Fc\text{–}C(Me)=CH\text{–}C_5H_4N\}W(CO)_5]$: triclinic, $P\bar{1}$; $a = 11.325(3)$, $b = 12.328(2)$, $c = 16.639(5)$ Å; $\alpha = 79.83(2)$, $\beta = 77.30(2)$, $\gamma = 82.043(14)°$; $Z = 4$; 5878 unique data; $R_1 = 0.035$, $wR_2 = 0.103$. Complex **7** $\cdot (CH_2Cl_2)_{0.5}$, $[\{Fc\text{–}CH=CH\text{–}C_5H_4N\}_2W(CO)_4 \cdot (CH_2Cl_2)_{0.5}]$: triclinic, $P\bar{1}$; $a = 10.290(2)$, $b = 11.751(4)$, $c = 16.328(4)$ Å; $\alpha = 88.071(14)$, $\beta = 83.502(14)$, $\gamma = 67.50(2)°$; $Z = 2$; 5054 unique data; $R_1 = 0.047$, $wR_2 = 0.125$. All of the complexes were fully characterised by ^1H and ^{13}C NMR, IR, UV–vis and luminescence spectroscopy, FAB mass spectrometry, and electrochemical measurements. The complexes show the expected spectroscopic and electrochemical features for both the ferrocenyl and substituted tungsten carbonyl chromophores. Although the individual molecules possess the necessary structural and electronic features required for second-order non-linear optical behaviour, the fact that the three crystallographically characterised complexes have centrosymmetric space groups precludes bulk solid-state measurements of NLO behaviour.

Keywords: Ferrocene; Tungsten; Pyridine; Crystal structure; Electrochemistry; UV–VIS Spectroscopy

1. Introduction

As part of our continuing study of interactions between remote metal centres linked by conjugated bridging ligands [1], we recently reported the synthesis of a variety of ferrocene derivatives with pendant pyridyl fragments to which additional metal fragments could be attached [2]. The ferrocenyl unit has been a particularly popular "building block" in such complexes due to its high chemical stability, chemically reversible redox behaviour, and ease of derivatisation [3]. This has led to its use as components in molecules as diverse as molecular ferromagnets [4], molecular sensors [5] and opto-electronic devices based on non-linear optical effects [6].

We describe here the preparation, structural characterisation and spectroscopic and electrochemical properties of a series of dinuclear and trinuclear complexes in which one or two pyridyl-substituted ferrocene derivatives (Fc-L) are attached to a tungsten carbonyl centre [7,8], giving complexes of the form $[(Fc\text{-}L)W(CO)_5]$ or *cis*-$[(Fc\text{-}L)_2W(CO)_4]$; the structural formulae of the complexes are given in Fig. 1. These complexes have a rich spectroscopic and electrochemical behaviour, containing two types of chromophore showing charge-transfer behaviour which may be beneficial for the construction of non-linear optical materials [3], and two types of redox-active centre whose redox potentials will allow assessment of long-range metal–metal interactions across the conjugated bridge.

* Corresponding author.

PII S0022-328X(96)06395-4

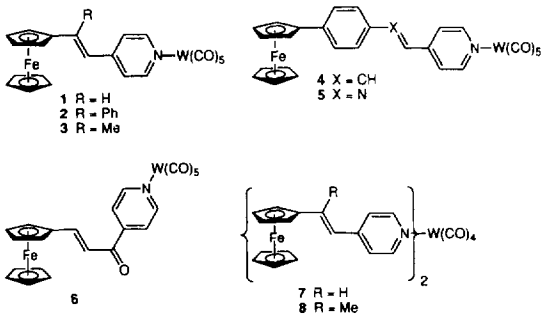

Fig. 1. Structural formulae of the new complexes.

2. Experimental

2.1. General details

The pyridyl-substituted ferrocene derivatives, denoted Fc-L, were prepared according to the published method [2]. $W(CO)_6$ was purchased from Strem Chemicals and used as received. Instrumentation used for routine spectroscopic analyses was as follows: NMR spectra, Jeol GX-270 or λ-300 spectrometers; FAB mass spectra (3-nitrobenzylalcohol matrix), a VG-Autospec; UV–vis spectra, Perkin-Elmer Lambda-2 or Lambda-19 spectrometers; IR spectra, a Perkin-Elmer FT-1600 spectrometer; luminescence spectra, a Perkin-Elmer LS50-B fluorimeter. Electrochemical measurements were made using the instrumentation and methods previously described [2]. Solvents for syntheses and electrochemical measurements were distilled from standard drying agents before use.

2.2. Syntheses of dinuclear complexes 1–6

$W(CO)_6$ (0.33 g, 0.93 mmol) was dissolved in dry THF (50 cm^3) in an N_2-purged Schlenk tube fitted with a condenser jacket. The solution was irradiated with a 500 W, medium-pressure mercury lamp whilst being stirred under N_2 for 1.5 h, until the solution became golden yellow. One equivalent (0.93 mmol) of the

Table 1
^1H and ^{13}C NMR data for the new complexes

	Proton NMR data	Carbon NMR data
1	8.63 (2H, d, J = 6.7, Py H^2/H^6), 7.27 (1H, d, J = 16, –CH=), 7.23 (2H, d, J = 6.7, Py H^3/H^5), 6.61 (1H, d, J = 16, –CH=), 4.55 (2H, t, J = 1.8, C_5H_4), 4.43 (2H, t, J = 1.8, C_5H_4), 4.16 (5H, s, Cp)	202.85 (*trans* CO), 198.24 (*cis* CO), 156.11 (Py) [a], 146.94 (Py), 136.62 (Py), 121.64 (–CH=), 121.03 (–CH=), 80.81 (1C, C_5H_4), 70.83 (2C, C_5H_4), 69.76 (5C, Cp), 68.17 (2C, C_5H_4)
2	8.38 (2H, d, J = 6.7, Py H^2/H^6), 7.47–7.51 (3H, m, Ph), 7.27–7.30 (2H, m, Ph), 6.76 (1H, s, –CH=), 6.62 (2H, d, J = 6.7, Py H^3/H^5), 4.43 (2H, d, J = 1.8, C_5H_4), 4.41 (2H, d, J = 1.8, C_5H_4), 4.16 (5H, s, Cp)	202.78 (*trans* CO), 199.10 (*cis* CO), 155.45 (Py), 151.45 (Ph) [b], 146.40 (Py), 138.78 (Py), 129.06 (–CH=), 128.68 (Ph), 128.46 (–C=), 124.46 (Ph), 119.29 (Ph), 85.70 (1C, C_5H_4), 70.61 (2C, C_5H_4), 69.98 (5C, Cp), 67.86 (2C, C_5H_4)
3	8.67–8.65 (2H, m, Py H^2/H^6), 7.18 (2H, d, J = 6.6, Py H^3/H^5), 6.58 (1H, S, –CH=), 4.53–4.55 (2H, m, C_5H_4), 4.39 (2H, m, C_5H_4), 4.15 (5H, s, Cp), 2.30 (3H, s, CH_3)	203.06 (*trans* CO), 199.41 (*cis* CO), 155.94 (Py), 147.75 (Py), 145.40 (Py), 125.28 (–CH=), 119.05 (–C=), 87.40 (1C, C_5H_4), 70.51 (2C, C_5H_4), 69.91 (5C, Cp), 66.892 (2C, C_5H_4), 18.00 (CH_3)
4	8.70 (2H, d, J = 6.8, Py H^2/H^6), 7.51 (4H, s, C_6H_4), 7.39 (1H, d, J = 16, –CH=), 7.32 (2H, d, J = 6.8, Py H^3/H^5), 7.02 (1H, d, J = 16, –CH=), 4.71 (2H, t, J = 1.8, C_5H_4), 4.38 (2H, t, J = 1.8, C_5H_4), 4.04 (5H, s, Cp)	202.94 (*trans* CO), 199.39 (*cis* CO), 156.45 (Py), 146.91 (Py), 142.04 (Ph), 136.20 (–CH=), 133.33 (Ph), 127.91 (Ph), 126.75 (Ph), 123.18 (–CH=), 122.56 (Py), 84.35 (1C, C_5H_4), 70.14 (5C, Cp), 70.02 (2C, C_5H_4), 66.99 (2C, C_5H_4)
5	8.93 (2H, d, J = 6.4, Py H^2/H^6), 8.57 (1H, s, –CH=), 7.75 (2H, dd, J = 6.6, Py H^3/H^5), 7.56 (2H, d, J = 8.8, phenyl), 7.29 (2H, d, J = 8.6 phenyl), 4.70 (2H, t, J = 1.8, C_5H_4), 4.38 (2H, t, J = 1.8, C_5H_4), 4.05 (5H, s, Cp)	202.97 (*trans* CO), 199.29 (4C, *cis* CO), 157.05 (Py), 154.19 (–CH=), 147.85 (Py), 144.75 (Ph), 140.48 (Ph), 127.21 (Ph), 124.13 (Py), 122.01 (Ph), 84.54 (1C, C_5H_4), 70.13 (5C, Cp), 69.89 (2C, C_5H_4), 66.97 (2C, C_5H_4)
6	9.00 (2H, d, J = 6.6, Py H^2/H^6), 7.83 (1H, d, J = 15, –CH=), 7.69 (2H, d, J = 6.8, Py H^3/H^5), 6.97 (1H, d, J = 15, –CH=), 4.66 (2H, m, C_5H_4), 4.61 (2H, m, C_5H_4), 4.21 (5H, s, Cp)	202.88 (*trans* CO), 199.22 (*cis* CO), 186.87 (ketonic C), 157.25 (Py), 151.17 (–CH=), 146.35 (Py), 123.85 (Py), 117.62 (–CH=), 78.70 (1C, C_5H_4), 72.97 (2C, C_5H_4), 70.55 (5C, Cp), 70.04 (2C, C_5H_4)
7	8.49 (4H, m, Py H^2/H^6), 7.16 (2H, d, J = 16, –CH=), 7.12 (4H, m, Py H^3/H^5), 6.49 (2H, d, J = 16, –CH=), 4.40 (4H, m, C_5H_4), 4.33 (4H, m, C_5H_4), 4.05 (10H, s, Cp)	213.90 (*trans* CO), 205.47 (*cis* CO), 154.95 (Py), 146.69 (Py), 136.21 (Py), 121.61 (–CH=), 121.56 (–CH=), 81.20 (2C, C_5H_4), 70.96 (4C, C_5H_4), 69.94 (10C, Cp), 68.29 (4C, C_5H_4)
8	8.52 (4H, d, J = 6.4, Py H^2/H^6), 7.06 (4H, d, J = 6.6, Py H^3/H^5), 6.48 (2H, s, –CH=), 4.34 (4H, m, C_5H_4), 4.28 (4H, m, C_5H_4), 4.05 (10H, s, Cp), 2.23 (6H, s, CH_3)	213.85 (*trans* CO), 205.47 (*cis* CO), 154.55 (Py), 147.31 (Py), 144.80 (Py), 125.02 (–CH=), 119.31 (–C=), 87.56 (2C, C_5H_4), 70.42 (4C, C_5H_4), 69.88 (10C, Cp), 66.83 (4C, C_5H_4)

[a] Py = pyridyl; [b] Ph = phenyl.

Table 2
Analytical, IR, mass spectroscopic and electrochemical data for the new complexes

	Elemental analysis [a]			ν(CO) (cm^{-1})	FABMS M^+	$E_{1/2}$ (V) (ΔE_p (mV))	
	%C	%H	%N			Fe-based	W-based
1	43.1 (43.1)	2.3 (2.5)	2.3 (2.3)	1891(m), 1927(s), 1971(sh), 2073(w)	613	0.08 (60)	0.68
2	47.8 (48.8)	2.6 (2.8)	1.9 (2.0)	1893(m), 1927(s), 1972(sh), 2070(w)	689	0.07 (120)	0.62
3	44.1 (44.0)	2.7 (2.7)	2.3 (2.2)	1892(m), 1930(s), 1975(sh), 2071(w)	627	0.06 (100)	0.76
4	46.5 (46.8)	2.6 (2.8)	1.8 (1.9) [b]	1893(m), 1928(s), 1975(m), 2071(w)	689	0.05 (120)	0.71
5	47.1 (47.0)	2.5 (2.6)	3.9 (4.0)	1900(m), 1929(s), 1974(m), 2070(w)	690	0.01 (150)	0.67
6	42.7 (43.1)	2.4 (2.4)	2.1 (2.2)	1902(m), 1930(s), 1974(w), 2071(w)	641	0.17 (130)	0.70
7	48.5 (48.8)	3.3 (3.3)	2.5 (2.9) [b]	1824(m), 1874(s), 1928(w), 2004(m)	874	— 0.08 (160) — [c]	
8	53.3 (53.3)	3.8 (3.8)	3.1 (3.1)	1824(m), 1874(s), 1928(w), 2004(m)	902	— 0.03 (190) — [c]	

[a] Calculated values in parentheses. [b] 0.5 molecules of CH_2Cl_2 per complex molecule required for elemental analysis.
[c] Two coincident ferrocene-based processes and one tungsten-based process all overlapping.

appropriate Fc-L was then added and the mixture was stirred for a further 1–2 h. The solvent was then evaporated in vacuo, and the residue chromatographed over alumina (Brockmann activity III) using gradient elution, with the eluent composition varying steadily from 1 : 1 CH_2Cl_2/hexane up to 5 : 1 CH_2Cl_2/hexane as required. Initially, traces of yellow $W(CO)_5(THF)$ eluted; the major red or purple band which followed was collected and the solvent evaporated in vacuo to give microcrystals of the product in yields of 60–90%. Recrystallisation was from CH_2Cl_2/hexane mixtures. Characterisation data for the complexes are given in Tables 1 and 2.

2.3. Syntheses of trinuclear complexes 7 and 8

Irradiation of $W(CO)_6$ (0.35 g, 1 mmol) in dry THF (50 cm^3) under N_2 was performed as above. To the resulting golden yellow solution was added 2.25 mmol of the appropriate Fc-L, and the mixture was then stirred for another 20 h with continuous UV-irradiation from the mercury lamp. After evaporation of the solvent

Table 3
Crystallographic data for **2**, **3** and **7** · $(CH_2Cl_2)_{0.5}$

	2	**3**	**7** · $(CH_2Cl_2)_{0.5}$
Empirical formula	$C_{28}H_{19}FeNO_5W$	$C_{23}H_{17}FeNO_5W$	$C_{38.5}H_{31}ClFe_2N_2O_4W$
Formula weight	689.1	627.1	916.7
Crystal system and space group	triclinic, $P\bar{1}$	triclinic, $P\bar{1}$	Triclinic, $P\bar{1}$
a (Å)	9.392(4)	11.325(3)	10.290(2)
b (Å)	12.115(3)	12.328(2)	11.751(4)
c (Å)	12.745(3)	16.639(5)	16.328(4)
α (°)	66.66(2)	79.83(2)	88.071(14)
β (°)	71.87(2)	77.30(2)	83.502(14)
γ (°)	81.40(2)	82.043(14)	67.50(2)
V (Å^3)	1264.9(7)	2218.5(9)	1812.3(8)
Z	2	4	2
ρ_{calc} (Mg m^{-3})	1.809	1.877	1.680
μ (Mo Kα) (mm^{-1})	5.155	5.868	4.071
Min/max transmission	0.228/0.714	0.195/0.609	0.114/0.334
F(000)	668	1208	902
Crystal size (mm^3)	0.5 × 0.5 × 0.1	0.5 × 0.4 × 0.05	0.6 × 0.5 × 0.2
2θ range (°)	3.6–46.5	2.5–46.5	2.5–46.5
Index ranges	$-10 \le h \le 10$, $-8 \le k \le 13$, $-14 \le l \le 14$	$-11 \le h \le 12$, $-13 \le k \le 12$, $-18 \le l \le 18$	$-11 \le h \le 10$, $-12 \le k \le 13$, $-15 \le l \le 18$
Reflections collected	4364	8187	7135
Unique data/restraints/parameters	3230/0/325	5878/0/559	5054/0/436
R_1, wR_2 [a,b]	0.032, 0.090	0.035, 0.103	0.047, 0.125
Weighting factors [b]	$a = 0.0616$; $b = 2.05$	$a = 0.0512$, $b = 5.41$	$a = 0.0663$, $b = 5.55$
Largest remaining peak/hole (e Å^{-3})	0.766, −0.871	1.132, −1.007	1.659, −0.976

[a] Structure was refined on F_o^2 using all data; the value of R_1 is given for comparison with older refinements based on F_o with a typical threshold of $F \ge 4\sigma(F)$.
[b] $wR_2 = [\Sigma[w(F_o^2 - F_c^2)^2]/\Sigma w(F_o^2)^2]^{1/2}$ where $w^{-1} = [\sigma^2(F_o^2) + (aP)^2 + bP]$ and $P = [\max(F_o^2, 0) + 2F_c^2]/3$.

in vacuo the residue was chromatographed as above using the same gradient elution technique with CH_2Cl_2/hexane mixtures of steadily increasing polarity. The first red fraction contained the dinuclear complex (ca. 45% yield); the second band contained the desired trinuclear complex which was isolated in ca. 40% yield. Characterisation data for the complexes are given in Tables 1 and 2.

2.4. X-ray crystallography

X-ray quality crystals of **2**, **3** and **7** · $(CH_2Cl_2)_{0.5}$ were grown from CH_2Cl_2/hexane mixtures. Suitable crystals were mounted on glass fibres on a Siemens SMART three-circle diffractometer fitted with a CCD-type area detector and using graphite-monochromated Mo Kα X-radiation ($\lambda = 0.71073$ Å). Details of the crystal parameters, data collection and refinement are given in Table 3. Data were corrected for Lorentz and polarisation effects, and for absorption effects by an

Table 4
Fractional atomic coordinates ($\times 10^4$) and equivalent isotropic thermal parameters (Å$^2 \times 10^3$) for **2**

Atom	x	y	z	U_{eq}
W(1)	1311(1)	2723(1)	−3434(1)	46(1)
C(1)	2368(8)	4213(7)	−4698(7)	64(2)
O(1)	2927(7)	5075(5)	−5443(6)	89(2)
O(2)	−697(7)	2905(6)	−5046(6)	82(2)
C(2)	28(9)	2835(6)	−4455(7)	58(2)
C(3)	2871(8)	1716(7)	−4235(7)	60(2)
O(3)	3742(7)	1211(6)	−4755(6)	89(2)
C(4)	−199(8)	3839(7)	−2789(6)	53(2)
O(4)	−1073(7)	4501(6)	−2473(6)	85(2)
C(5)	87(8)	1290(7)	−2181(7)	60(2)
O(5)	−661(7)	511(5)	−1467(6)	88(2)
Fe(1)	7491(1)	3194(1)	1747(1)	57(1)
C(11)	8180(19)	4802(12)	1531(20)	135(6)
C(12)	7345(24)	4247(15)	2679(18)	151(7)
C(13)	5843(15)	4085(11)	2580(16)	121(5)
C(14)	5988(15)	4599(9)	1385(15)	111(4)
C(15)	7366(20)	5000(9)	771(15)	134(5)
C(21)	8503(7)	2303(7)	639(7)	61(2)
C(22)	9349(8)	2144(7)	1435(7)	64(2)
C(23)	8428(8)	1602(7)	2610(7)	66(2)
C(24)	7013(7)	1421(6)	2538(6)	55(2)
C(25)	7032(7)	1843(6)	1333(6)	48(1)
C(26)	5787(7)	1809(5)	883(6)	47(1)
C(27)	5905(7)	2163(6)	−272(6)	52(2)
C(31)	4365(7)	1352(6)	1835(5)	49(2)
C(32)	3263(9)	2125(10)	2152(8)	82(2)
C(33)	1979(10)	1647(18)	3079(12)	124(5)
C(34)	1841(13)	429(20)	3642(9)	140(7)
C(35)	2924(13)	−307(13)	3320(10)	126(5)
C(36)	4180(10)	127(9)	2436(8)	82(3)
N(41)	2857(6)	2498(5)	−2289(5)	47(1)
C(42)	4220(8)	2992(6)	−2763(6)	55(2)
C(43)	5191(8)	2863(6)	−2115(6)	56(2)
C(44)	4829(7)	2208(6)	−889(5)	47(1)
C(45)	3434(7)	1686(6)	−407(6)	54(2)
C(46)	2515(7)	1846(6)	−1105(6)	55(2)

Table 5
Fractional atomic coordinates ($\times 10^4$) and equivalent isotropic thermal parameters (Å$^2 \times 10^3$) for **3**

Atom	x	y	z	U_{eq}
W(1)	2958(1)	10163(1)	3327(1)	49(1)
C(1)	1512(9)	11336(7)	3487(6)	63(2)
O(1)	707(7)	11982(6)	3562(5)	100(2)
C(2)	2992(11)	9911(9)	4561(6)	82(3)
O(2)	3092(12)	9853(10)	5233(5)	145(4)
C(3)	4072(9)	11325(8)	3160(7)	78(3)
O(3)	4712(8)	11987(7)	3053(7)	124(3)
C(4)	2971(7)	10495(6)	2089(6)	54(2)
O(4)	2981(6)	10741(6)	1388(4)	82(2)
C(5)	4449(8)	9013(6)	3163(5)	52(2)
O(5)	5276(6)	8392(6)	3093(5)	90(2)
Fe(1)	−2975(1)	4340(1)	3784(1)	48(1)
C(11)	−2962(9)	5545(8)	2781(5)	74(3)
C(12)	−4154(8)	5424(8)	3194(5)	68(2)
C(13)	−4396(8)	4318(8)	3203(6)	66(2)
C(14)	−3325(9)	3756(9)	2794(6)	76(3)
C(15)	−2432(9)	4532(10)	2530(6)	81(3)
C(21)	−3280(7)	4602(7)	4985(5)	54(2)
C(22)	−3351(8)	3464(7)	4953(5)	66(2)
C(23)	−2225(9)	3034(7)	4520(6)	68(2)
C(24)	−1449(7)	3901(6)	4275(5)	56(2)
C(25)	−2098(6)	4873(6)	4563(4)	47(2)
C(26)	−1660(6)	5986(6)	4426(4)	44(2)
C(27)	−463(7)	6062(6)	4156(5)	51(2)
C(28)	−2601(7)	6931(6)	4575(6)	61(2)
N(31)	1694(6)	8814(5)	3549(4)	51(2)
C(32)	586(7)	8882(6)	4047(5)	59(2)
C(33)	−163(7)	8051(7)	4256(5)	57(2)
C(34)	210(6)	7048(6)	3949(5)	47(2)
C(35)	1356(7)	6986(6)	3427(5)	60(2)
C(36)	2048(7)	7856(6)	3253(5)	57(2)
W(2)	2293(1)	4702(1)	1375(1)	49(1)
C(6)	3789(9)	3629(7)	1075(6)	68(2)
O(6)	4597(8)	2985(7)	918(6)	114(3)
C(7)	2196(11)	5113(8)	167(7)	80(3)
O(7)	2058(12)	5334(9)	−514(5)	143(4)
C(8)	2336(8)	4258(6)	2589(6)	58(2)
O(8)	2344(7)	3986(6)	3291(4)	89(2)
C(9)	1243(9)	3513(7)	1467(6)	70(2)
O(9)	627(7)	2831(6)	1517(6)	100(2)
C(10)	757(8)	5734(6)	1671(6)	60(2)
O(10)	−115(7)	6289(6)	1830(6)	104(3)
Fe(2)	8293(1)	10255(1)	1539(1)	45(1)
C(41)	9805(8)	10194(8)	2033(7)	74(3)
C(42)	8763(11)	10590(8)	2571(7)	82(3)
C(43)	7938(9)	9778(10)	2799(5)	76(3)
C(44)	8468(9)	8890(8)	2401(6)	73(3)
C(45)	9609(9)	9130(8)	1941(6)	75(3)
C(51)	8424(6)	10291(7)	297(4)	48(2)
C(52)	8502(7)	11365(7)	461(5)	58(2)
C(53)	7426(7)	11680(6)	1023(5)	60(2)
C(54)	6664(6)	10801(6)	1188(5)	50(2)
C(55)	7276(6)	9933(6)	751(4)	43(2)
C(56)	6819(6)	8874(6)	746(4)	42(2)
C(57)	5613(7)	8830(6)	931(4)	48(2)
C(58)	7748(7)	7936(7)	514(6)	63(2)
N(61)	3471(6)	6099(5)	1241(4)	48(2)
C(62)	4618(7)	5918(7)	1377(6)	62(2)
C(63)	5342(7)	6767(7)	1282(6)	65(2)
C(64)	4932(7)	7866(6)	1025(4)	46(2)
C(65)	3745(6)	8039(6)	882(5)	50(2)
C(66)	3069(7)	7167(6)	997(5)	54(2)

empirical method based on multiple measurements of equivalent data. The structures were solved by conventional direct methods (SHELXTL) and were refined by the full-matrix least-squares method on all F^2 data (SHELX93) using Silicon Graphics Indigo R4000 or Indy computers [9]. All non-hydrogen atoms were refined anisotropically; hydrogen atoms were included in calculated positions and refined with fixed isotropic thermal parameters. Atomic coordinates are given in Tables 4–6, and selected bond lengths and angles are assembled in Tables 7–9 respectively. Complex **3** contains two independent molecules in the asymmetric unit; complex $\mathbf{7}\cdot(CH_2Cl_2)_{0.5}$ contains one molecule of CH_2Cl_2 in the unit cell which is disordered over the inversion centre. The two chlorine atoms are ordered, one either side of the inversion centre, but the carbon atom was found to be disordered over two positions with 50% site occupancy in each.

Table 6
Fractional atomic coordinates ($\times 10^4$) and equivalent isotropic thermal parameters ($Å^2 \times 10^3$) for $\mathbf{7}\cdot(CH_2Cl_2)_{0.5}$

Atom	x	y	z	U_{eq}
W(1)	−5573(1)	5642(1)	2528(1)	52(1)
Fe(1)	−2144(1)	−1362(1)	−1658(1)	69(1)
Fe(2)	2386(1)	950(1)	6015(1)	63(1)
C(1)	−7194(9)	6129(7)	1895(5)	60(2)
O(1)	−8217(8)	6434(9)	1564(5)	102(2)
C(2)	−6595(9)	4712(8)	3215(6)	65(2)
O(2)	−7278(8)	4309(7)	3626(5)	97(2)
C(3)	−4847(9)	6771(8)	1828(6)	67(2)
O(3)	−4541(8)	7455(7)	1405(5)	98(2)
C(4)	−6606(11)	7098(9)	3234(6)	69(2)
O(4)	−7209(8)	7972(7)	3634(5)	94(2)
C(11)	−3082(12)	−2591(12)	−1741(11)	107(4)
C(12)	−3674(13)	−1863(13)	−1028(9)	103(4)
C(13)	−4254(11)	−612(13)	−1281(10)	103(4)
C(14)	−4036(14)	−589(13)	−2135(11)	115(5)
C(15)	−3311(15)	−1818(13)	−2421(10)	112(4)
C(21)	−989(12)	−337(9)	−2030(7)	87(3)
C(22)	−246(13)	−1596(11)	−2305(8)	99(4)
C(23)	−34(10)	−2345(10)	−1625(8)	87(3)
C(24)	−619(9)	−1615(8)	−900(7)	73(2)
C(25)	−1197(9)	−352(9)	−1161(6)	71(2)
C(26)	−1927(9)	748(8)	−641(7)	74(3)
C(27)	−2069(9)	792(9)	165(6)	69(2)
N(31)	−4276(7)	3983(6)	1710(4)	57(2)
C(32)	−4025(11)	4074(9)	902(6)	77(3)
C(33)	−3327(12)	3070(9)	380(6)	84(3)
C(34)	−2823(8)	1889(7)	677(5)	60(2)
C(35)	−3058(10)	1810(9)	1514(6)	75(2)
C(36)	−3766(10)	2829(8)	1994(6)	71(2)
C(41)	2188(27)	−80(15)	5107(9)	139(7)
C(42)	3518(22)	−457(18)	5243(16)	160(10)
C(43)	3587(20)	−868(11)	6083(17)	154(9)
C(44)	2155(15)	−627(13)	6370(9)	106(4)
C(45)	1371(14)	−156(11)	5773(10)	106(4)
C(51)	2583(9)	2540(8)	5629(6)	69(2)
C(52)	3373(10)	2090(9)	6295(7)	79(3)
C(53)	2433(11)	1998(11)	6978(7)	89(3)
C(54)	1061(11)	2409(10)	6736(6)	80(3)
C(55)	1116(9)	2757(8)	5891(5)	64(2)
C(56)	−65(9)	3134(8)	5410(6)	67(2)
C(57)	−96(9)	3589(8)	4658(6)	64(2)
N(61)	−3682(7)	4924(6)	3253(4)	57(2)
C(62)	−2420(8)	4976(7)	2986(5)	59(2)
C(63)	−1261(8)	4559(8)	3420(5)	63(2)
C(64)	−1326(8)	4020(7)	4175(5)	60(2)
C(65)	−2576(11)	3886(10)	4440(6)	79(3)
C(66)	−3713(7)	4326(6)	3975(4)	76(3)
Cl(1)	−997(7)	5783(6)	576(4)	271(5)
C(100)	376(7)	5171(6)	323(4)	125(10)

3. Results and discussion

3.1. Syntheses and characterisation

Substitution of carbonyl ligands of $W(CO)_6$ by pyridines (py) to give $[W(CO)_5(py)]$ and *cis*-$[W(CO)_4(py)_2]$ is a well-known reaction which occurs with either thermal or photochemical stimulus [7,8,10,11]. We found that displacement of one CO ligand to give the dinuclear complexes **1–6** was facile, but substitution of a second ligand to give the trinuclear complexes **7** and **8** required prolonged reaction times and still afforded substantial amounts of mono-substituted product; fortunately chromatographic separation was straightforward. All complexes were satisfactorily characterised by their FAB mass spectra, ^1H and ^{13}C NMR spectra, elemental analyses, and characteristic pattern of carbonyl bands in the IR spectra [11] (Tables 1 and 2).

A few points are worth noting. In every case the pyridyl H^2 and H^6 protons are equivalent by ^1H NMR at room temperature, as are C^2 and C^6 by ^{13}C NMR. The same applies to H^3/H^5 and C^3/C^5. This implies rapid rotation of the pyridyl ring with respect to the vinyl group to which it is attached, since if the pyridyl ring were planar with the rest of the conjugated system and static, it could not have two-fold symmetry. The same is true of the ferrocenyl group; the substituted cyclopentadienyl ring displays two doublets in the proton NMR spectrum, and three signals in the ratio 2:2:1 in the ^{13}C NMR spectrum. Secondly, cleavage of the N–W bonds occurs easily under the conditions of the FAB mass spectra; although a weak molecular ion was seen in every case, the strongest signal usually arose from the ferrocenyl-pyridine ligand following dissociation from the tungsten centre.

3.2. Crystal structures

The crystal structures of **2**, **3** and $\mathbf{7}\cdot(CH_2Cl_2)_{0.5}$ shown in Figs. 2–4 respectively (see also Tables 4–9) are essentially as expected and confirm the formulations of the complexes. In all cases the tungsten centres are very close to ideal octahedral geometry and the W–C–O bonds are near-linear. The W–N(pyridyl) bond lengths

(2.25–2.28 Å) lie in the expected range [7,12]. The expected *trans* effect is present, with the W–C bonds *trans* to the pyridyl ligands (1.95–1.99 Å) being significantly shorter than the other W–C bonds (2.01–2.05 Å). The ferrocenyl fragments are also unremarkable. The two significant features of each of the structures which are worthy of comment are related to the bridging fragment between the metal centres. These are (i) the conformation and extent of distortion of the vinylic bridging fragments, and (ii) the orientation of the coordinated pyridyl rings at the tungsten centre with respect to the ancillary carbonyl ligands.

Starting with the trinuclear complex **7**, the conjugated arms linking the ferrocenyl and tungsten fragments are nearly planar. The carbon atoms of the double bonds are in each case virtually coplanar with the cyclopentadienyl ring to which they are attached. The plane of the pyridyl ring containing N(31) is twisted by only 3° from the plane of the vinyl-cyclopentadienyl fragment to which it is attached; in contrast, in the other ferrocenyl-pyridine ligand the equivalent dihedral angle is 14°. The fact that both ligands in **7** are only minimally distorted from planarity is due to the lack of steric crowding around the *trans*-disubstituted double bonds. In complex **3**, the additional methyl substitutent on the double bond results in greater distortions away from planarity. Complex **3** has two independent molecules in the unit cell. For the first of these [containing W(1)] the plane containing atoms C(26), C(27) and C(28), i.e. the double bond and its methyl substituent, is twisted by 15° with respect to the plane of the cyclopentadienyl ring C(21)–C(25). The pyridyl ring [N(31)–C(36)] is twisted in the opposite sense by 23° with respect to the plane C(26)–C(28); the result is that the plane of this pyridyl ring is only twisted by 8° with respect to that of the cyclopentadienyl ring. In the second independent molecule [containing W(2)] the distortions are large, with the analogous dihedral twists being 24° (double bond with respect to cyclopentadienyl ring) and then, in the same sense, 31° (pyridyl ring with respect to double bond). The significant difference between the two independent molecules of **3** indicates that quite substantial distortions of the conjugated bridge are relatively easy to achieve and may be imposed by crystal packing constraints in addition to steric factors within the molecule. Complex **2** has the most highly hindered bridge, with a phenyl substitutent attached to the double bond. In this case the pyridyl ring is twisted by 10° with respect to the plane containing C(21)–C(27); however, the phenyl substitutent is nearly perpendicular to this plane, with a dihedral twist of 81°. This twisting of the phenyl ring out of the plane of the bridge arises from two potentially unfavourable steric interactions (with the pyridyl ring and with the ferrocenyl group) which would otherwise be a problem, and this in turn allows the pyridyl ring to remain virtually coplanar with the rest of the bridge.

The orientation of the coordinated pyridyl rings with respect to the tungsten fragment is defined by the angles between the pyridyl plane and the planes consisting of the W, N, and other ancillary ligands. Thus for **2**, the pyridyl ring is at an angle of 73° to the W–N–C(2)–C(3)–C(4) mean plane, and 17° to the orthogonal W–N–C(1)–C(2)–C(5) plane. For the two independent

Table 7
Selected bond lengths (Å) and angles (°) for **2**

W(1)–C(2)	1.987(8)	W(1)–C(1)	2.019(8)
W(1)–C(4)	2.024(8)	W(1)–C(5)	2.036(8)
W(1)–C(3)	2.049(8)	W(1)–N(41)	2.280(5)
C(1)–O(1)	1.155(10)	O(2)–C(2)	1.136(9)
C(3)–O(3)	1.148(9)	C(4)–O(4)	1.155(9)
C(5)–O(5)	1.154(9)		
Fe(1)–C(14)	2.041(9)	Fe(1)–C(25)	2.045(7)
Fe(1)–C(13)	2.017(10)	Fe(1)–C(12)	2.025(10)
Fe(1)–C(21)	2.033(7)	Fe(1)–C(24)	2.031(7)
Fe(1)–C(15)	2.051(10)	Fe(1)–C(23)	2.030(7)
Fe(1)–C(22)	2.032(7)	Fe(1)–C(11)	2.031(11)
C(25)–C(26)	1.466(9)	C(26)–C(27)	1.333(9)
C(26)–C(31)	1.498(9)	C(27)–C(44)	1.445(9)
C(2)–W(1)–C(1)	89.7(3)	C(2)–W(1)–C(4)	87.7(3)
C(1)–W(1)–C(4)	87.0(3)	C(2)–W(1)–C(5)	87.1(3)
C(1)–W(1)–C(5)	175.4(2)	C(4)–W(1)–C(5)	89.7(3)
C(2)–W(1)–C(3)	89.9(3)	C(1)–W(1)–C(3)	88.5(3)
C(4)–W(1)–C(3)	174.8(2)	C(5)–W(1)–C(3)	94.8(3)
C(2)–W(1)–N(41)	176.6(2)	C(1)–W(1)–N(41)	91.3(3)
C(4)–W(1)–N(41)	95.7(2)	C(5)–W(1)–N(41)	92.1(3)
C(3)–W(1)–N(41)	86.9(2)	C(27)–C(26)–C(25)	123.0(6)
C(27)–C(26)–C(31)	122.9(6)	C(25)–C(26)–C(31)	114.1(6)
C(26)–C(27)–C(44)	131.5(6)		

molecules of **3**, these angles are 30° and 61° [for the W(1) molecule], and 29° and 62° [for the W(2) molecule]. Finally, for **7**, the relevant angles are 78° and 12° [for the pyridyl ring containing N(61)] and 55° and 35° [for the pyridyl ring containing N(31)]. W(dπ)-to-pyridine(π*) back-bonding would be maximised when these angles are 0° and 90°, although steric interactions between the pyridyl ring and the carbonyl ligands would be minimised by 45° angles in which the plane of the pyridyl ring is "staggered" with respect to the carbonyl ligands rather than "eclipsed".

3.3. Electrochemical behaviour

The dinuclear complexes **1–6** contain one ferrocene and one [$W(CO)_5$(py)]-type fragment, both of which are redox active (Fig. 5, Table 2). In CH_2Cl_2 all of these complexes display a chemically reversible ferrocene/ferrocenium couple (the cathodic and anodic peak currents are equal and the waves are symmetric). The peak-to-peak separations are, however, significantly greater than the ideal value of 60 mV for a fully reversible one-electron process. This may be ascribed to

Table 8
Selected bond lengths (Å) and angles (°) for **3**

W(1)–C(3)	1.982(9)	W(1)–C(4)	2.024(10)
W(1)–C(2)	2.030(10)	W(1)–C(1)	2.032(10)
W(1)–C(5)	2.052(8)	W(1)–N(31)	2.271(6)
C(1)–O(1)	1.125(11)	C(2)–O(2)	1.138(12)
C(3)–O(3)	1.131(10)	C(4)–O(4)	1.151(10)
C(5)–O(5)	1.123(10)	Fe(1)–C(15)	2.022(9)
Fe(1)–C(11)	2.027(8)	Fe(1)–C(21)	2.028(8)
Fe(1)–C(12)	2.036(8)	Fe(1)–C(25)	2.037(7)
Fe(1)–C(22)	2.039(8)	Fe(1)–C(24)	2.040(7)
Fe(1)–C(14)	2.042(9)	Fe(1)–C(23)	2.049(8)
Fe(1)–C(13)	2.055(8)	C(25)–C(26)	1.487(10)
C(26)–C(27)	1.341(10)	C(26)–C(28)	1.482(11)
C(27)–C(34)	1.474(10)		
W(2)–C(9)	1.977(9)	W(2)–C(8)	2.007(9)
W(2)–C(7)	2.007(11)	W(2)–C(6)	2.028(10)
W(2)–C(10)	2.029(9)	W(2)–N(61)	2.273(6)
C(6)–O(6)	1.142(11)	C(7)–O(7)	1.158(13)
C(8)–O(8)	1.159(11)	C(9)–O(9)	1.146(10)
C(10)–O(10)	1.129(10)	Fe(2)–C(44)	2.028(8)
Fe(2)–C(42)	2.028(9)	Fe(2)–C(51)	2.031(7)
Fe(2)–C(45)	2.033(8)	Fe(2)–C(53)	2.036(8)
Fe(2)–C(43)	2.040(9)	Fe(2)–C(41)	2.043(8)
Fe(2)–C(55)	2.045(7)	Fe(2)–C(52)	2.045(7)
Fe(2)–C(54)	2.046(7)	C(55)–C(56)	1.471(10)
C(56)–C(57)	1.339(10)	C(56)–C(58)	1.495(11)
C(57)–C(64)	1.472(10)		
C(3)–W(1)–C(4)	88.0(4)	C(3)–W(1)–C(2)	88.7(4)
C(4)–W(1)–C(2)	176.7(4)	C(3)–W(1)–C(1)	89.6(4)
C(4)–W(1)–C(1)	87.7(3)	C(2)–W(1)–C(1)	91.6(4)
C(3)–W(1)–C(5)	88.8(4)	C(4)–W(1)–C(5)	92.3(3)
C(2)–W(1)–C(5)	88.3(4)	C(1)–W(1)–C(5)	178.4(3)
C(3)–W(1)–N(31)	178.5(3)	C(4)–W(1)–N(31)	93.4(3)
C(2)–W(1)–N(31)	89.9(4)	C(1)–W(1)–N(31)	90.9(3)
C(5)–W(1)–N(31)	90.7(3)	C(27)–(C26)–C(28)	125.4(7)
C(27)–C(26)–C(25)	118.0(7)	C(28)–C(26)–C(25)	116.5(6)
C(26)–C(27)–C(34)	129.6(7)		
C(9)–W(2)–C(8)	89.0(4)	C(9)–W(2)–C(7)	88.9(4)
C(8)–W(2)–C(7)	177.9(4)	C(9)–W(2)–C(6)	90.0(4)
C(8)–W(2)–C(6)	90.2(4)	C(7)–W(2)–C(6)	90.4(4)
C(9)–W(2)–C(10)	88.0(4)	C(8)–W(2)–C(10)	90.1(4)
C(7)–W(2)–C(10)	89.3(4)	C(6)–W(2)–C(10)	177.9(3)
C(9)–W(2)–N(61)	178.3(3)	C(8)–W(2)–N(61)	92.4(3)
C(7)–W(2)–N(61)	89.6(3)	C(6)–W(2)–N(61)	90.9(3)
C(10)–W(2)–N(61)	91.1(3)	C(57)–C(56)–C(55)	117.9(7)
C(57)–C(56)–C(58)	125.3(7)	C(55)–C(56)–C(58)	116.8(6)
C(56)–C(57)–C(64)	128.6(7)		

Table 9
Selected bond lengths (Å) and angles (°) for $7 \cdot (CH_2Cl_2)_{0.5}$

W(1)–C(1)	1.949(9)	W(1)–C(2)	2.022(9)
W(1)–C(4)	1.963(10)	W(1)–N(61)	2.258(7)
W(1)–C(3)	2.021(10)	W(1)–N(31)	2.268(7)
C(1)–O(1)	1.164(11)	C(2)–O(2)	1.139(11)
C(3)–O(3)	1.154(11)	C(4)–O(4)	1.154(11)
Fe(1)–C(21)	2.029(10)	Fe(2)–C(42)	2.004(14)
Fe(1)–C(13)	2.034(11)	Fe(2)–C(44)	2.015(13)
Fe(1)–C(24)	2.035(9)	Fe(2)–C(41)	2.020(13)
Fe(1)–C(11)	2.035(11)	Fe(2)–C(43)	2.025(13)
Fe(1)–C(25)	2.036(8)	Fe(2)–C(45)	2.025(11)
Fe(1)–C(22)	2.037(11)	Fe(2)–C(51)	2.029(9)
Fe(1)–C(15)	2.038(11)	Fe(2)–C(55)	2.042(9)
Fe(1)–C(23)	2.039(10)	Fe(2)–C(54)	2.042(9)
Fe(1)–C(14)	2.040(12)	Fe(2)–C(53)	2.046(10)
Fe(1)–C(12)	2.045(12)	Fe(2)–C(52)	2.055(9)
C(55)–C(56)	1.439(12)	C(25)–C(26)	1.464(12)
C(56)–C(57)	1.322(12)	C(26)–C(27)	1.308(14)
C(57)–C(64)	1.479(12)	C(27)–C(34)	1.458(12)
C(1)–W(1)–C(4)	88.4(4)	C(3)–W(1)–N(61)	94.3(3)
C(1)–W(1)–C(3)	89.0(3)	C(1)–W(1)–N(31)	93.7(3)
C(4)–W(1)–C(3)	85.3(4)	C(4)–W(1)–N(31)	177.0(3)
C(1)–W(1)–C(2)	84.1(3)	C(3)–W(1)–N(31)	92.7(3)
C(4)–W(1)–C(2)	89.3(4)	C(2)–W(1)–N(31)	93.0(3)
C(3)–W(1)–C(2)	171.3(3)	N(61)–W(1)–N(31)	83.0(2)
C(1)–W(1)–N(61)	175.5(3)	C(27)–C(26)–C(25)	126.5(10)
C(4)–W(1)–N(61)	94.9(3)	C(26)–C(27)–C(34)	126.1(9)
C(57)–C(56)–C(55)	126.3(8)	C(56)–C(57)–C(64)	126.3(8)

a combination of uncompensated solution resistance and slightly slow electron-transfer kinetics; unsubstituted ferrocene under the same conditions gave ΔE_p values of 100–120 mV. The redox potentials are all slightly positive with respect to the ferrocene/ferrocenium couple (Fc/Fc^+), which is to be expected given the slightly electron-withdrawing nature of the conjugated side-arms. However, these redox potentials are very similar to those of the free ferrocenyl-pyridine ligands [2]; i.e. coordination of a neutral $\{W(CO)_5\}$ moiety to the pyridyl group does not have a significant effect on the redox potential of the ferrocene centre. In contrast, coordination of cationic $\{Mo(NO)(Tp^*)Cl\}^+$ fragments [Tp^* = hydrotris(3,5-dimethylpyrazolyl)borate] to the same ligands resulted in shifts to more positive potentials of between 50 and 100 mV of the ferrocene-centred redox couples, as a consequence of the additional electron-withdrawing effect of the positive charge [2]. In addition, complexes **1–6** all display the expected irreversible tungsten-centred oxidation at ca. 0.7 V vs. Fc/Fc^+ [7,8]. These do not vary much, in keeping with the similar nature of the $\{W(CO)_5N\}$ fragments of **1–6**.

Replacement of an additional carbonyl ligand by a pyridyl group in the trinuclear complexes **7** and **8**

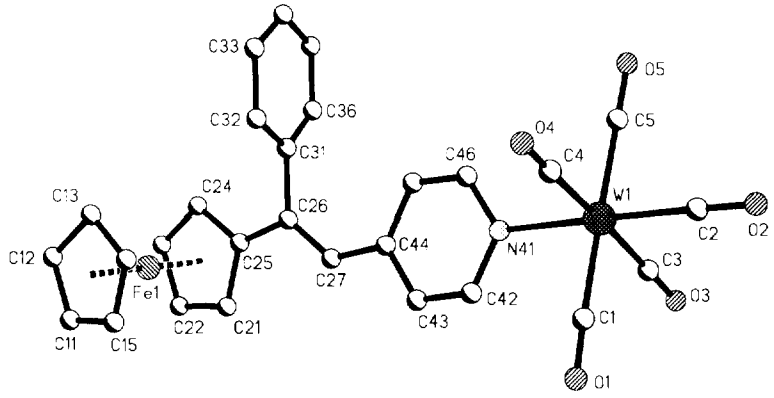

Fig. 2. Crystal structure of complex **2**.

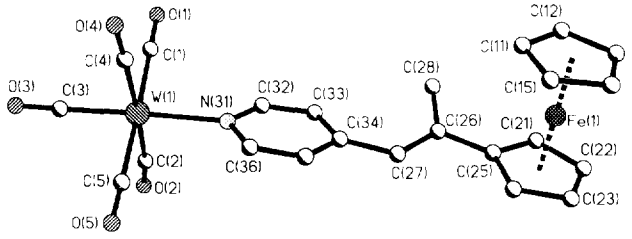

Fig. 3. Crystal structure of complex **3** (only one of the two independent molecules is shown; the other is similar).

increases the electron density of the tungsten centre, which therefore oxidises more easily. The cathodic shift of these processes by ca. 0.6 V means that they now occur at approximately the same potentials as the ferrocene-centred processes, and both cyclic and square-wave voltammetric studies on **7** and **8** reveal just a single broad wave which presumably comprises both (chemically reversible) ferrocene/ferrocenium couples and the (chemically irreversible) tungsten-centred oxidation (Fig. 5).

No ligand-centred reduction processes were apparent within the limits of the solvent window, in contrast to complexes such as $[\{W(CO)_5\}_2(\mu\text{-}4,4'\text{-bipyridine})]$ in which two reversible ligand-centred reductions occur [7,12].

3.4. Electronic spectra

The electronic absorption and emission spectra are summarised in Table 10. Assignment of the electronic spectral peaks is complicated by the overlap of transitions associated with the ferrocenyl and the tungsten chromophores.

Unsubstituted ferrocene exhibits two bands at 325 and 440 nm in the electronic spectrum, which have been

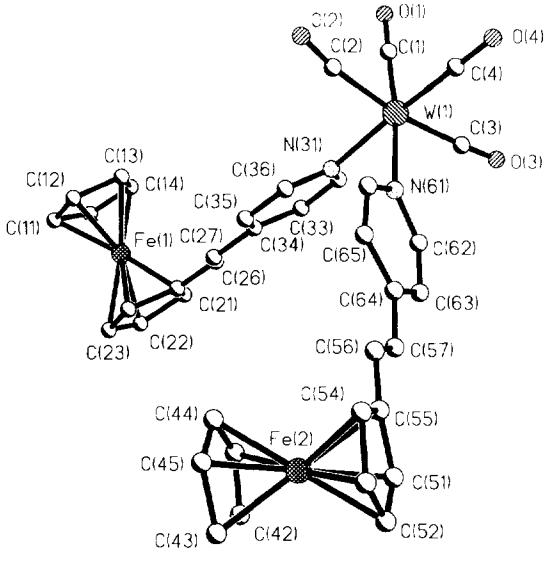

Fig. 4. Crystal structure of complex $7\cdot(CH_2Cl_2)_{0.5}$.

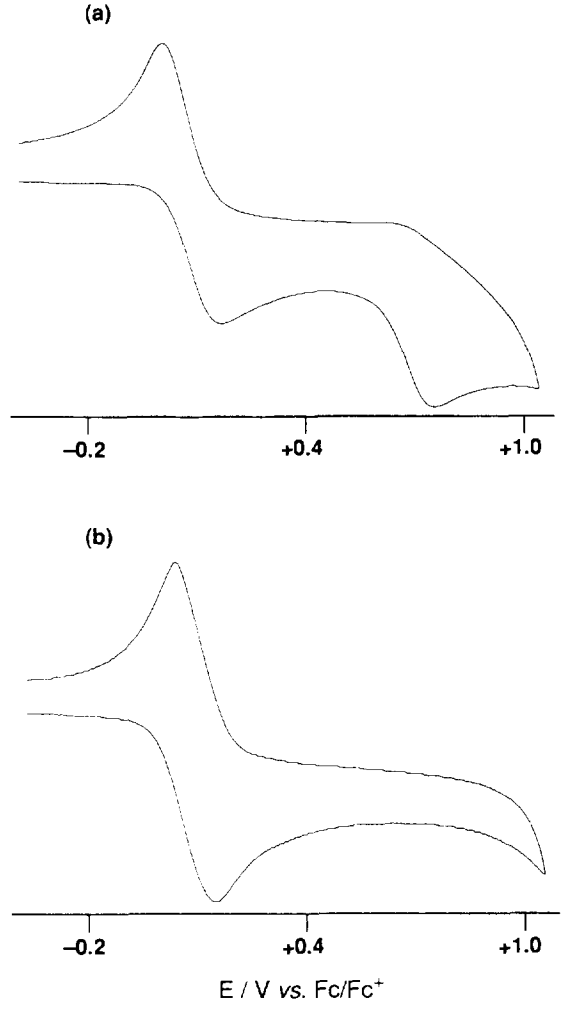

Fig. 5. Cyclic voltammograms of (a) **1** and (b) **7**, recorded in CH_2Cl_2 at a Pt-bead working electrode with a scan rate of 0.2 V s^{-1}.

assigned to $^1A_{2g} \rightarrow {}^1E_{2g}$ and $^1A_{1g} \rightarrow {}^1E_{1g}$ ligand–field (d–d) transitions [13]. Upon substitution of a cyclopentadienyl ring with conjugated acceptor groups, it is expected that (i) cyclopentadienyl orbitals will shift to lower energy, and (ii) there will be increased mixing of ligand orbitals with the metal d-orbitals, resulting in an

Table 10
Electronic spectral and luminescence data for the new complexes.

Complex	λ_{max} (nm) [$10^{-3}\varepsilon$ (dm^3 mol^{-1} cm^{-1})] [a]			λ_{em} (nm) ($10^4\Phi$) [a,b]
1	494 (4.0)	394 (18)	330 (18)	530 (1.9)
2	505 (2.4)	394 (15)	336 (12)	530 (1.3)
3	≈ 500 (sh)	386 (13)	322 (13)	533 (0.8)
4	≈ 480 (sh)	399 (21)	354 (22)	523 (1.3)
5	≈ 500 (sh)	402 (17)	289 (sh)	537 (1.3)
6	551 (4.1)	397 (11)	332 (14)	537 (1.9)
7	478 (13)	416 (14)	321 (36)	522 (1.8)
8	470 (sh)	411 (18)	314 (36)	522 (2.8)

[a] Spectra measured in CH_2Cl_2 at room temperature. [b] Quantum yields referenced to $[Ru(bipy)_3][PF_6]_2$ in aerated water ($\Phi = 0.028$).

increased intensity for the transitions since they will have some metal-to-ligand charge-transfer (MLCT) character. The free ferrocenyl-pyridine ligands were shown to have two transitions (with $\varepsilon < 5000$ $dm^3\ mol^{-1}\ cm^{-1}$) between ca. 350 and 500 nm in accordance with these expectations [2], and an intense $\pi \rightarrow \pi^*$ transition based on the conjugated side-arm at around 300 nm with $\varepsilon > 10^4$ $dm^3\ mol^{-1}\ cm^{-1}$. $\{W(CO)_5(py)\}$-type chromophores undergo a d–d transition close to 400 nm which is relatively invariant, and a $W \rightarrow L(\pi^*)$ MLCT transition which can lie anywhere between 350 and 550 nm depending on the nature of the substituents on the pyridyl ligand [7]. In the region 300–550 nm therefore up to five intense, overlapping transitions may be expected. In fact most of the spectra in CH_2Cl_2 show two strong maxima at ca. 300 and 400 nm, both with $\varepsilon \approx 10^4$ $dm^3\ mol^{-1}\ cm^{-1}$, and a weaker peak near 500 nm which is sometimes only discernible as a shoulder. By comparison with the spectra of the free ferrocenyl-pyridine ligands [2], the highest-energy band (around 300 nm) is the $\pi \rightarrow \pi^*$ transition of the conjugated pyridyl arm, and the weaker lowest-energy band (around 500 nm) is a ferrocenyl-based MLCT process. The remaining ferrocenyl-based MLCT (around 380 nm), the tungsten-based d–d transition (around 400 nm), and the $W \rightarrow L(\pi^*)$ MLCT process (variable position) are all overlapping and not individually resolved. In more polar solvents the maximum at around 400 nm moves to higher energy, and splits into two. Fig. 6 shows the spectra of **1** in hexane and DMSO; the single peak at 406 nm in hexane becomes two (barely resolved) peaks at ca. 360 and 380 nm in DMSO.

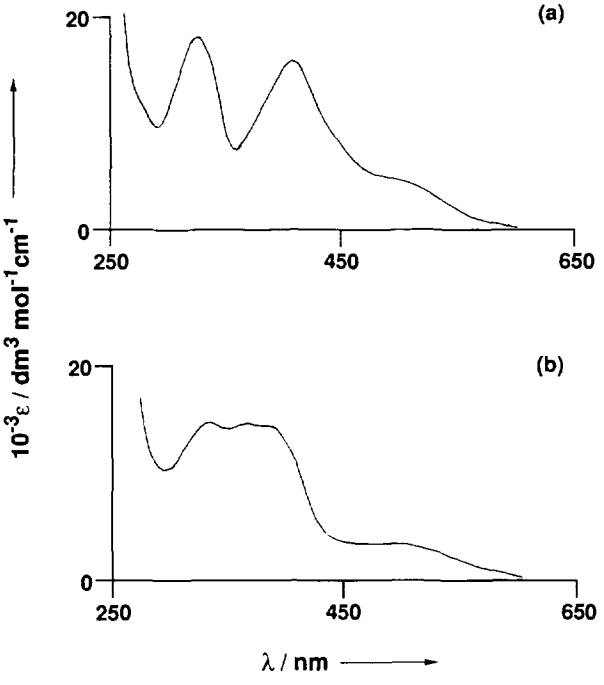

Fig. 6. Electronic spectra of **1** in (a) hexane and (b) DMSO.

Owing to their obvious negative solvatochromism these must be the two (ferrocenyl-centred and tungsten-centred) MLCT transitions. The tungsten-based d–d transition, the only one unaccounted for, is likely to be weaker and therefore buried under these two intense charge-transfer processes.

3.5. Luminescence spectra

All of the complexes have a very weak emission at ca. 530 nm, with quantum yields of the order of 10^{-4} in aerated CH_2Cl_2 at room temperature (Table 10). By analogy with other species containing the same chromophore, this emission is assigned to the lowest-energy $W \rightarrow L(\pi^*)$ MLCT excited state [12]. Since the absorption maximum of the $W \rightarrow L(\pi^*)$ MLCT transition is not clear in the electronic spectra, excitation was performed at 450 nm, a region of the spectrum close to where the $W \rightarrow L(\pi^*)$ MLCT transition would be expected. Excitation into the more strongly-absorbing maxima at around 400 and 300 nm did not significantly increase the intensity of the emission, possibly because although the complex absorbs more light at these wavelengths, most of it is into transitions other than the $W \rightarrow L(\pi^*)$ MLCT which do not result in luminescence.

The virtual invariance of the emission maxima indicates that in all of the complexes this excited state is nearly invariant in energy. In other $\{W(CO)_5(py)\}$-type complexes this emission varies in wavelength from 550 to 700 nm depending on the nature of the substituents on the pyridyl ligand, but we observed no such variation in the emission maximum. It is not possible to see how the ligand substituents affected the energy of the $W \rightarrow L(\pi^*)$ MLCT transitions, as these were not clearly defined in the electronic spectra. The final noteworthy point about the emission spectra is that the $W \rightarrow L(\pi^*)$ MLCT excited states do not appear to be significantly quenched by the ferrocenyl fragment, despite the known ability of ferrocene to quench the luminescence of other d^6 complexes [14].

4. Conclusions

We have prepared and fully characterised a series of complexes in which one or two ferrocenyl-pyridine ligands (electron-donors) have been attached to an electron-deficient tungsten carbonyl fragment via a conjugated bridge. These complexes therefore have the basic architectural and electronic properties necessary to exhibit second-order non-linear optical behaviour, and indeed other complexes based on attachment of electron donors to tungsten carbonyl centres via pyridyl ligands have been shown to have significantly high values of the molecular hyperpolarisability β [15]. Although the

complexes that we characterised by X-ray methods (**2**, **3** and **7**) all crystallise in a centrosymmetric space group and cannot therefore show second-order non-linear properties in the bulk solid state, the β values for the individual molecules may still be substantial. These measurements will be the subject of a separate report.

References

[1] (a) A. Wlodarczyk, J.P. Maher, J.A. McCleverty and M.D. Ward, *J. Chem. Soc., Chem. Commun.*, (1995) 2397. (b) A.J. Amoroso, A.M.W. Cargill Thompson, J.P. Maher, J.A. McCleverty and M.D. Ward, *Inorg. Chem.*, *34* (1995) 4828. (c) J.P. Maher, J.A. McCleverty, M.D. Ward and A. Wlodarczyk, *J. Chem. Soc., Dalton Trans.*, (1994) 143. (d) A. Das, J.C. Jeffery, J.P. Maher, J.A. McCleverty, E. Schatz, M.D. Ward and G. Wollermann, *Inorg. Chem.*, *32* (1993) 2145. (e) A.M.W. Cargill Thompson, D. Gatteschi, J.A. McCleverty, J.A. Navas, E. Rentschler and M.D. Ward, *Inorg. Chem.*, *35* (1996) 2701.

[2] M.M. Bhadbhade, A. Das, J.C. Jeffery, J.A. McCleverty, J.A. Navas Badiola and M.D. Ward, *J. Chem. Soc., Dalton Trans.*, (1995) 2769.

[3] D.W. Bruce and D. O'Hare (eds.), *Inorganic Materials*, Wiley, Chichester, 1994.

[4] (a) C. Kollmar, M. Conty and D. Kahn, *J. Am. Chem. Soc.*, *113* (1991) 7994. (b) K.M. Chi, J.C. Calabrese, W.M. Reiff and J.S. Miller, *Organometallics*, *10* (1991) 668. (c) K.S. Narayan, B.G. Morin, J.S. Miller and A.J. Epstein, *Phys. Rev. B*, *46* (1992) 6195.

[5] (a) E.C. Constable, *Angew. Chem., Int. Engl.*, *30* (1991) 407. (b) R.W. Wagner, P.A. Brown, T.E. Johnson and J.S. Lindsey, *J. Chem. Soc., Chem. Commun.*, (1991) 1463. (c) M.C.B. Colbert, S.L. Ingham, J. Lewis, N.J. Long and P.R. Raithby, *J. Chem. Soc., Dalton Trans.*, (1994) 2215. (d) P.D. Beer, C. Blackburn, J.F. McAleer and H. Sikanyika, *Inorg. Chem.*, *29* (1990) 378. (e) P.D. Beer, *Chem. Soc. Rev.*, *18* (1989) 409.

[6] (a) M.W. Laidlaw, R.G. Denning, T. Verbiest, E. Chanchard and A. Persoons, *Nature*, *363* (1993) 58. (b) B.J. Coe, C.J. Jones, J.A. McCleverty, D. Bloor, P.V. Kolinsky and R.J. Jones, *J. Chem. Soc., Chem. Commun.*, (1989) 1485. (c) B.J. Coe, J.-D. Foulon, T.A. Hamor, C.J. Jones, J.A. McCleverty, D. Bloor, G.H. Cross and T.L. Axon, *J. Chem. Soc., Dalton Trans.*, (1994) 3427. (d) D.R. Kanis, M.A. Ratner and T.J. Marks, *J. Am. Chem. Soc.*, *114* (1992) 10338. (e) D.R. Kanis, M.A. Ratner and T.J. Marks, *Chem. Rev.*, *94* (1994) 195. (f) J.C. Calabrese, L.-T. Cheng, J.C. Green, S.R. Marder and W. Tam, *J. Am. Chem. Soc.*, *113* (1991) 7227. (g) S.R. Marder, J.W. Perry, B.G. Tiemann and W.P. Schaefer, *Organometallics*, *10* (1991) 1896. (h) A. Togni and G. Rihs, *Organometallics*, *12* (1993) 3368.

[7] J.T. Lin, S.-S. Sun, J.J. Wu, L. Lee, K.-J. Lin and Y.F. Huang, *Inorg. Chem.*, *34* (1995) 2323.

[8] M.M. Zulu and A.J. Lees, *Inorg. Chem.*, *27* (1988) 1139.

[9] SHELXTL 5.03 program system, Siemens Analytical X-Ray Instruments, Madison, WI, 1995.

[10] W. Strohmeier, K. Gerlach and G. Matthias, *Z. Naturforsch.*, *15b* (1960) 621.

[11] C.S. Kraihanzel and F.A. Cotton, *Inorg. Chem.*, *2* (1963) 533.

[12] J.T. Lin, P.S. Huang, T.Y.R. Tsai, C.Y. Liao, L.H. Tseng, Y.S. Wen and F.K. Shi, *Inorg. Chem.*, *31* (1992) 4444.

[13] Y.S. Sohn, D.N. Hendrickson and H.B. Gray, *J. Am. Chem. Soc.*, *93* (1971) 3603.

[14] J.-C. Chambron, C. Coudret and J.-P. Sauvage, *New. J. Chem.*, *16* (1992) 361.

[15] (a) L.-T. Cheng, W. Tam, G.R. Meredith and S.R. Marder, *Mol. Cryst. Liq. Cryst.*, *189* (1990) 137. (b) L.-T. Cheng, W. Tam and D.F. Eaton, *Organometallics*, *9* (1990) 2857.